DOI: 10.1002/chem.201001173

Electrochemical and Electrochemiluminescence Determination of Cancer Cells Based on Aptamers and Magnetic Beads

Caifeng Ding, Ying Ge, and Shusheng Zhang*[a]

Abstract: The electrochemical and electrochemiluminescence (ECL) detection of cell lines of Burkitt's lymphoma (Ramos) by using magnetic beads as the separation tool and high-affinity DNA aptamers for signal recognition is reported. Au nanoparticles (NPs) bifunctionalized with aptamers and CdS NPs were used for electrochemical signal amplification. The anodic stripping voltammetry technology employed for the analysis of cadmium ions dissolved from CdS NPs on the aggregates provided a means to quantify the amount of the target cells. This electrochemical method could respond down to 67 cancer cells per mL with a linear calibration range from 1.0×10^2 to 1.0×10^5 cells mL^{-1}, which shows very high sensitivity. In addition, the assay was able to differentiate between target and control cells based on the aptamer used in the assay, indicating the wide applicability of the assay for diseased cell detection. ECL detection was also performed by functionalizing the signal DNA, which was complementary to the aptamer of the Ramos cells, with tris(2,2-bipyridyl) ruthenium. The ECL intensity of the signal DNA, replaced by the target cells from the ECL probes, directly reflected the quantity of the amount of the cells. With the use of the developed ECL probe, a limit of detection as low as 89 Ramos cells per mL could be achieved. The proposed methods based on electrochemical and ECL should have wide applications in the diagnosis of cancers due to their high sensitivity, simplicity, and low cost.

Keywords: aptamers · cancer · electrochemistry · luminescence · nanoparticles

Introduction

Early and accurate diagnosis is essential for the effective and ultimately successful treatment of cancers. It has been reported that very sensitive monitoring of cancer cells could provide an easier and more effective way to monitor the progression of the disease.[1–5] Thus, identification and detection of cancer cells is fundamental to therapy and a means of monitoring the relevant biological processes of cancers. However, many of the current commercially available diagnosis methods are expensive, time-consuming, and requiring advanced instrumentation though they have a high detection rate.[6–11] Therefore, a more cost-effective method requiring simple or no instrumentation yet still providing great sensitivity and accuracy would be ideal for point of care diagnosis.

The most recent efforts in cancer cell detection have focused on biosensors with good sensitivity and selectivity, as well as rapid and easy operation. Ju and co-workers developed a series of cytosensors based on nanomaterials.[12] A strategy to detect P-glycoprotein in the cell membrane and to quantify number of cells by using an electrochemical immunoassay was constructed by the adsorption of colloidal gold nanoparticles (Au NPs) on a methoxysilyl-terminated, butyrylchitosan-modified glassy carbon electrode. Another novel architecture was designed by combining the biocompatibility of chitosan and the excellent conductivity of carbon nanofibers. The impedance of electronic transduction was related to the amount of the adhered K562 cells with a detect limitation of 1×10^3 cells mL^{-1}.[13] Based on the specific recognition of integrin receptors on a cell surface to arginine–glycine–aspartic acid–serine-functionalized single-walled carbon nanotubes, a novel electrochemical cytosensing strategy was designed. The cytosensor could respond down to 620 cells mL^{-1} of BGC-832 human gastric carcinoma (BCG) cells.[14] They recently developed an in situ analysis of cell-surface carbohydrates by electrochemical elemen-

[a] Dr. C. Ding, Y. Ge, Prof. S. Zhang
State Key Laboratory Base of Eco-chemical Engineering
College of Chemistry and Molecular Engineering
Qingdao University of Science and Technology
Qingdao 266042 (China)
Fax: (+86) 532-84022750
E-mail: shushzhang@126.com

Supporting information for this article is available on the WWW under http://dx.doi.org/10.1002/chem.201001173.

tal analysis of CdS quantum dots (QDs). The proposed method exhibited a sensitive response to the K562 cell from 1.0×10^{2} to 1.0×10^{7} cells mL^{-1}.[15] Although these electrochemical strategies are simple and sensitive, there is still a limitation due to complex processes required for the adherence of the target cells. In addition, it is difficult to differentiate diseased cells from healthy cells.

Aptamers are single-stranded nucleic acids that bind very specifically with protrin molecular or cellular targets, and thus are clear alternatives to long-established antibody-based diagnostic or biotechnological products for research, diagnostics, and therapy.[16–23]An in vitro process identifying DNA sequences with strong affinities toward intact tumor cells referred to as tumor cell SELEX[24] was used to select aptamers with high specificity toward target cancer cell lines developed by Tan's group.[25,26] The aptamers selected were used to detect cancer cells due to their ability to distinguish one cell type from numerous other cell types. They have developed a novel two-nanoparticle assay with aptamers as the molecular-recognition element for the rapid collection and detection of one kind of leukemia cells and then multiple cancer cells. Aptamer-conjugated magnetic NPs and aptamer-conjugated fluorescent NPs were employed for selective targeting in cell extraction and sensitive cellular detection, respectively. The detection limit was determined to be approximately 250 cells with a dynamic range covering more than 2 orders of magnitude. To increase signal strength and enhance binding affinity, the molecular assembly of aptamers on Au–Ag nanorods (NRs) and Au NP surfaces also significantly improves the binding affinity for cancer cells through simultaneous multivalent interactions with cell-membrane receptors. As determined by flow cytometric measurements, an enhancement in fluorescence signal in excess of 300-fold is obtained for the NR–aptamer-labeled cells compared with those labeled by individual aptamer probes.[27,28] They also constructed a cellular model and applied this aptamer–receptor interaction to estimate receptor densities and distributions on the cell surface.[29] The cellular internalization of one of the selected aptamers, sgc8, which binds human protein tyrosine kinase-7 on cell surfaces was also studied. This study indicates that sgc8 is a promising agent for cell-type specific intracellular deliveries.[30] By using aptamers, the selectivity of these methods is improved significantly. However, the instruments of fluorescent imaging and flow cytometry used for cellular detection are more expensive than electrochemical apparatus. In addition, the color of the complicated samples, such as fetal bovine serum, will make the determination difficult. Therefore, further sample preparation to remove any colored species may be necessary for any colorimetric detection.

Herein, electrochemical and electrochemiluminescence (ECL) assays are described for the rapid detection of cell lines of Burkitt's lymphoma (Ramos) by using high-affinity DNA aptamers for signal recognition. Streptavidin (or carboxyl)-coated magnetic beads (MBs) were used as both the separation tool and the immobilization matrix. The high performance of these two assays allowed measurements down to 100 Ramos cells per mL to be achieved. In addition, with the high sensitivity and simple process, the electrochemical method also demonstrated the capacity to reproducibly detect target cells from complex mixtures and FBS. Through taking advantage of the unique properties of the aptamers and MBs, we have developed an assay that has excellent selectivity between target and control cells. Being able to distinguish cancerous from noncancerous samples quickly and without any costly or complex instrumentation would be a very powerful tool for point of care diagnostics and even allow for the large-scale screening of particular diseases prior to more costly and invasive procedures.

Results and Discussion

The electrochemical principle used for the amplified sensing of target cells is shown in Scheme 1. The capture DNA **1** was tethered to MBs through a binding event between the streptavidin and biotin. The aptamer and the linker DNA tagged with CdS NPs were immobilized on the surface of Au NPs through a thiol anchor to construct the Au nanoprobes. After partial hybridization between the capture DNA **1** and the aptamer, the formation of a MB–Au–CdS biocomplex was accomplished. In the presence of the target cells the double-stranded (ds) DNA dehybrized. Au nanoprobes, were released from the biocomplex and assembled on the surface of the cancer cell through the recognition of the aptamer to its target on the cell-membrane surface. The concentration of target cells was monitored based on the concentration of dissolved Cd^{2+}, which was quantified by anodic stripping voltammetry (ASV). Since a single Au NP could be loaded with 38 CdS NPs (see Section 4 in the Supporting Information for more details), a significant amplification for the detection of target cell was obtained.[31]

Fluorescence imaging and TEM were adopted to demonstrate the conjugation between the cancers cells and the Au nanoprobes, as shown in Figure 1. In the fluorescence imaging experiment, CdTe NPs with stronger fluorescence intensities were employed to replace CdS NPs to be tagged on the surface of the Au NPs through the linker DNA. After the target cells were incubated with the prepared biocomplex, washed by magnetic extraction, and then dispersed in the analysis solution, the fluorescent signal was clear and strong (Figure 1 A). However, no fluorescence could be seen in the cancer cells that were not incubated with the biocomplex (Figure 1 B).

To verify that the nanoprobes were assembling on the surface of the target cells, TEM images of the target Ramos cells and control K562 cells after incubation with the MB–Au–CdS biocomplex were also taken. The assay protocol given in reference [28] was observed for both target and control cells followed by deposition onto a copper grid for TEM imaging. The samples were then allowed to dry before images were recorded. Based on the TEM images, the Au nanoprobes appeared on the surface of the target cells (Figure 1 C) and not on the surface of the control cells (Fig-

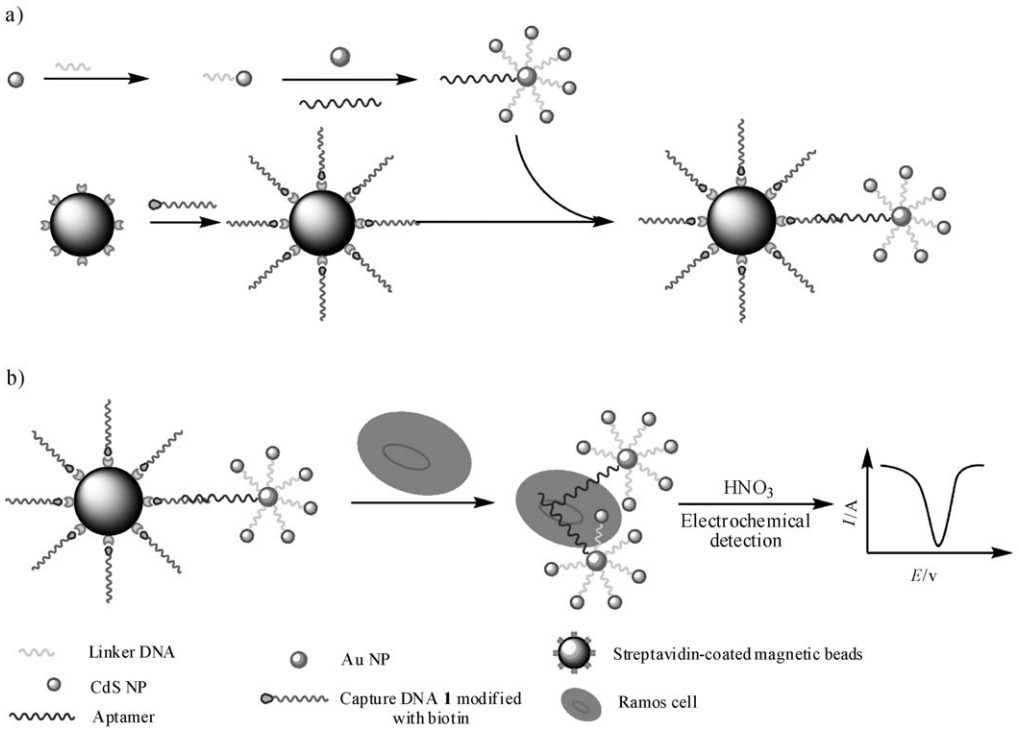

Scheme 1. A schematic illustration of a) the preparation of the MB–Au–CdS biocomplex and b) the electrochemical determination of cancer cells.

ure 1 D). These results indicated that the aptamers on the Au nanoprobes caused the assembly of the Au nanoprobes on the target cell surface.

To demonstrate the principle of the present assay, the selectivity was determined as to whether the MB–Au–CdS biocomplex could differentiate between target and control cells. The differential pulse voltammograms of Cd^{2+} dissolved from the same amount of target cells and control cells incubated with the same concentration of the MB–Au–CdS biocomplex are shown in Figure 2 A. The results established that the electrochemical signal of the target cells (Figure 2 A, curve c) was significantly higher than the same amount of control cells (curve b), which was approximately the same as the blank solution (curve a). These results indicated that the Au nanoprobes were dissociated from the MB–Au–CdS biocomplex and bound selectively to the target cells.

To truly evaluate the assay, more complicated samples were analyzed to determine whether the assay could be useful for actual samples. To accomplish this, the assay was also used to determine cancer cells in the cell media (FBS solution). In these experiments, target cells were added to FBS and then the same MB–Au–CdS biocomplex solution was added. After incubation, separation, and dissolution, the electrochemical signals were recorded by using the electrochemical analyzer. The DPV peak currents at about 0.62 V was plotted in Figure 2 B. For comparison, the signals of the same amount of control cells in FBS were also measured. The target cells in FBS clearly showed a significantly higher signal than the control cells in the FBS, indicating that the assay functioned as expected in even complex environments. As an additional control, cells of each type were also incubated with the MB–Au–CdS biocomplex solution modified with a nontarget aptamer sequence (random DNA). The sequence had no specificity for either cell type and produced no noticeable change in electrochemical signals of both cells versus the blank solution. This indicated that the Au nanoprobe must be able to dissociate from the MB–Au–CdS biocomplex and bind to the surface of the target cells due to the recognition of the aptamer to its target on the cell membrane surface.

Under the optimal conditions (see Section 3 in the Supporting Information), the DPV peak current was proportional to the cell concentration ranging from 1.0×10^2 to 1.0×10^5 cells mL^{-1} with a correlation coefficient, R, of 0.998 ($n=11$) (Figure 3). The regression equation, I (μA) = $0.3915+1.6148\times10^{-4}C$ (cells mL^{-1}), was used, in which I was the current intensity, and C was the cell concentration. A series of eleven duplicate measurements of 200 cells mL^{-1} were used for estimating the precision, and the relative standard deviation (RSD) was 5.3 %; this shows good reproducibility. The detection limit for cell concentration was calculated to be 67 cells mL^{-1} at 3σ. The low detection limit was ascribed to the signal amplification of Au NPs and the ASV analysis of Cd^{2+} dissolved from the Au nanoprobes.

The proposed method and other techniques using nanoparticles for the determination of cancer cells are compared in Table S2 in the Supporting Information. From these results we can see that the current method is more sensitive than others.

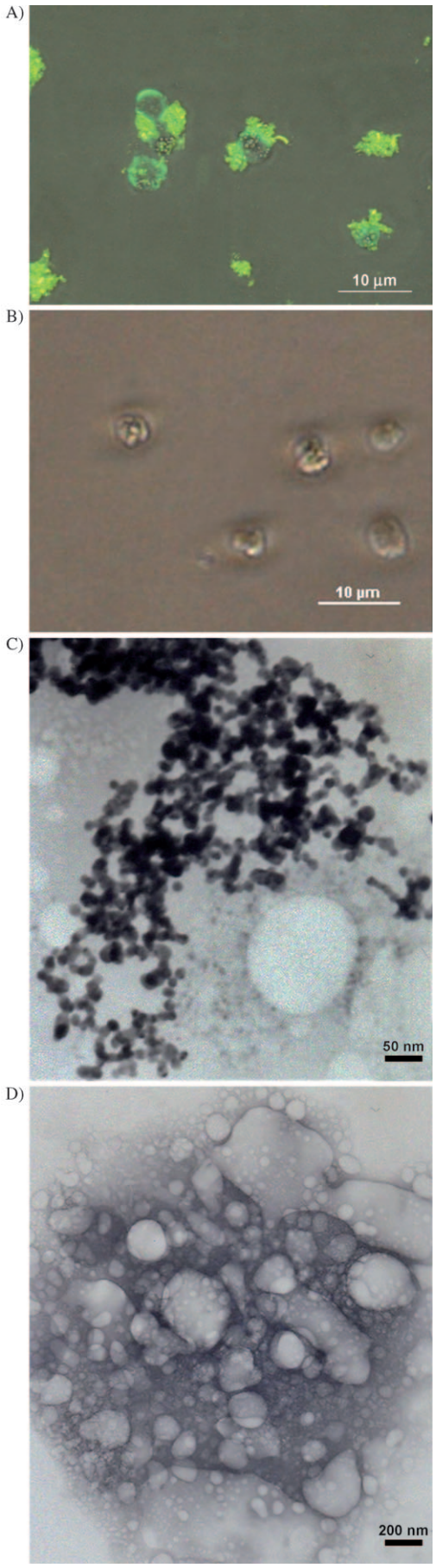

Figure 1. The fluorescence image of cancer cells conjugated with Au nanoprobes (A), cancer cells only (B), and the TEM images of target (C) and control cells (D) mixed with the MB-Au-CdS biocomplex. The concentration of cells in all samples was 15000 cells mL^{-1}.

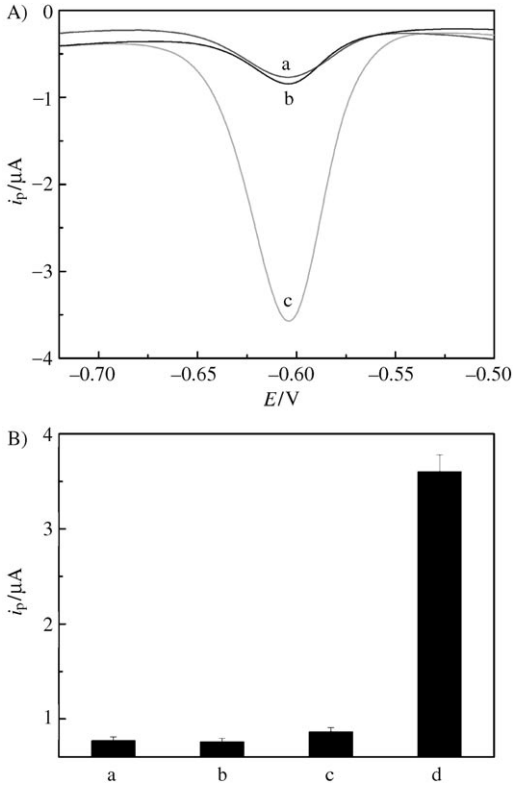

Figure 2. A) Difference responses for electrochemical detection of cells between the Ramos cells and K562 cells in PBS; a) without cells, b) with the K562 cells, and c) with the Ramos cells. B) Bar graph showing the change of intensity between the Ramos cells and K562 cells in FBS; a) without cells, b) with the K562 cells, c) with a nontarget aptamer sequence, and d) with the Ramos cells. The concentration of cells was 15000 cells mL^{-1}.

The ECL experimental concept is schematically shown in Scheme 2. Prior to the tests, MB–Ru biocomplex was synthesized first by functionalizing MBs with ECL nanoprobes by hybridization between the aptamers modified on the surface of the MBs and the signal DNA labeled with tris(2,2-bipyridyl) ruthenium (TBR). ECL nanoprobes were responsible for the ECL detection, and MBs modified with aptamers were used to recognize the Ramos cells and used as a separation tool. For cell analysis, the MB–Ru biocomplex was incubated with Ramos cells for 2 h at room temperature. The aptamers recognized the Ramos cells with high affinity and dehybridized with the signal DNA. Thus, the ECL probes were released from the MB–Ru biocomplexes and dispersed in the solution. Then the solution containing the ECL probes was separated from the mixture with a magnetic field. Afterwards, the gold electrode modified with capture DNA **2**, which was complementary to the signal DNA, was immersed in the above solution for 1 h at 37 °C to form ds-

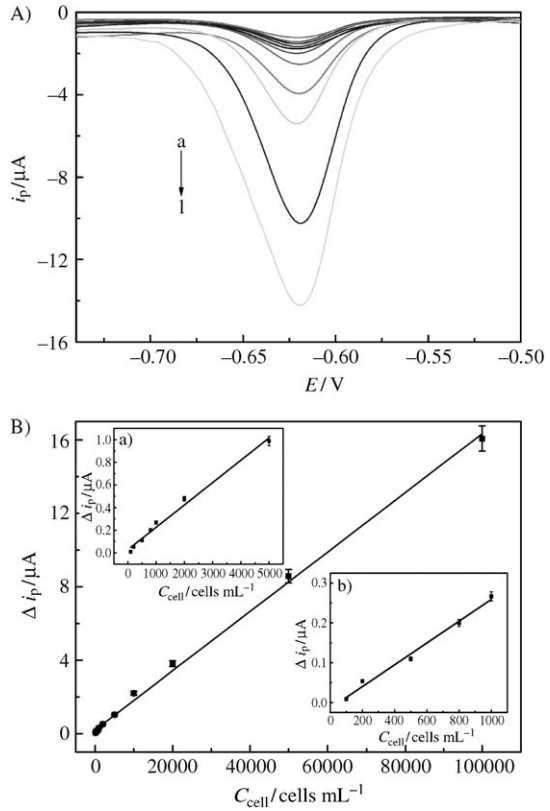

Figure 3. Dose responses (A) and calibration curves (B) for electrochemical detection of cells. The concentrations of the cells in A: 0 (a), 100 (b), 200 (c), 500 (d), 800 (e), 1000 (f), 2000 (g), 5000 (h), 10000 (i), 20000 (j), 50000 (k), and 100000 cells mL^{-1} (l). The concentrations of the cells in B were the same as those in A without the blank. (insets: amplifications of the 100 to 5000 (a) and 100 to 1000 cells mL^{-1} (b) regions).

DNA. Subsequently, the resulting gold electrode was immersed into ECL assay buffer for subsequent ECL detection.

Figure 4 shows the kinetic curves of ECL assays obtained upon different concentrations of target cells. A control experiment, carried out by mixing MB–Ru biocomplex with

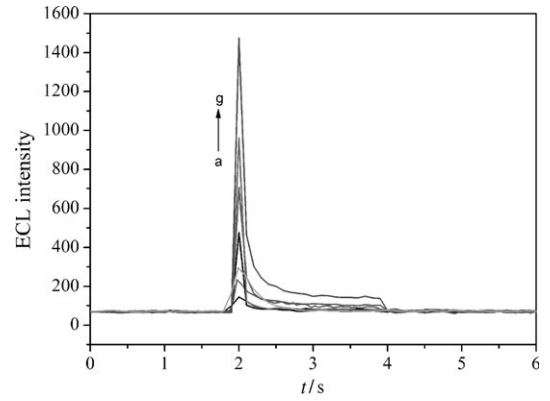

Figure 4. ECL profiles of the cytosensor in different concentrations of Ramos cells. Cell concentrations: a) 0, b) 100, c) 300, d) 500, e) 1000, f) 2000, and g) 3000 cells mL^{-1}. The voltage of the ECL was set at 1.0 V. Scan rate: 100 mV s.$^{-1}$

K562 cells in the absence of target cells, clearly demonstrates that little unspecific binding occurs (Figure 4, curve a). It is clear that ECL intensity increases with an increasing target concentration compared with the control.

As shown in Figure 5, the target cells could be quantitatively measured over a large concentration variation from 100 to 50000 cells mL^{-1}. A plateau effect was reached above

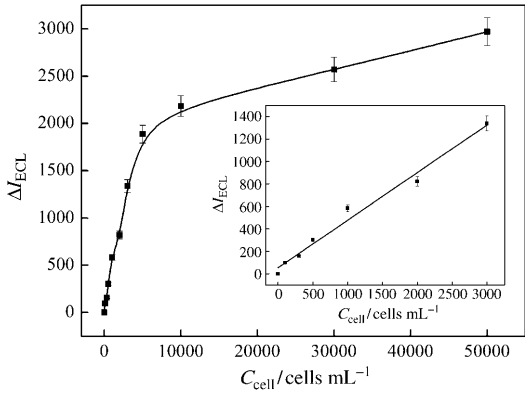

Figure 5. Calibration curves for ECL detection of cells. Concentrations of the cells: 0, 100, 300, 500, 1000, 2000, 3000, 5000, 10000, 30000, 50000 cells mL^{-1}. (inset: amplifications of the 0 to 3000 cells mL^{-1} region).

concentrations of 3000 Ramos cells per mL, which may be due to depletion of ECL nanoprobes loaded on the MBs. Under the optimized test conditions, the linear range and detection limit of the designed ECL strategy for the Ramos cells were measured as shown in the inset of Figure 5. The results showed that the increased ECL intensity was related to the concentration of the Ramos cells in the range from 100 to 3000 cells mL^{-1}. The regression equation, $I_{ECL} = 55.04 + 0.42C$ (cells mL^{-1}), with a regression coefficient of 0.992 was used. To investigate accuracy of the proposed assay, the relative standard deviation (RSD) was determined by measuring the ECL signal of 300 cells mL^{-1} with eleven replicates; the RSD value was 6.9%, which shows good reproducibility. The detection limit was 89 cells mL^{-1}, which was almost the same as that obtained by electrochemical approaches based on the signal amplification of NPs. It could be predicted that a lower detection limit could be obtained due to the signal amplification of NPs in the ECL detection method.

Conclusion

The present study demonstrates the analysis of cancer cells by means of electrochemical and ECL methods based on aptamers for the specific recognition event and MBs as a separation tool. By utilizing the unique amplification of Au NPs and the excellent selectivity of aptamers, the electrochemical assay could detect Ramos cells with high sensitivity. It was clear that the detection limit of the ECL strategy

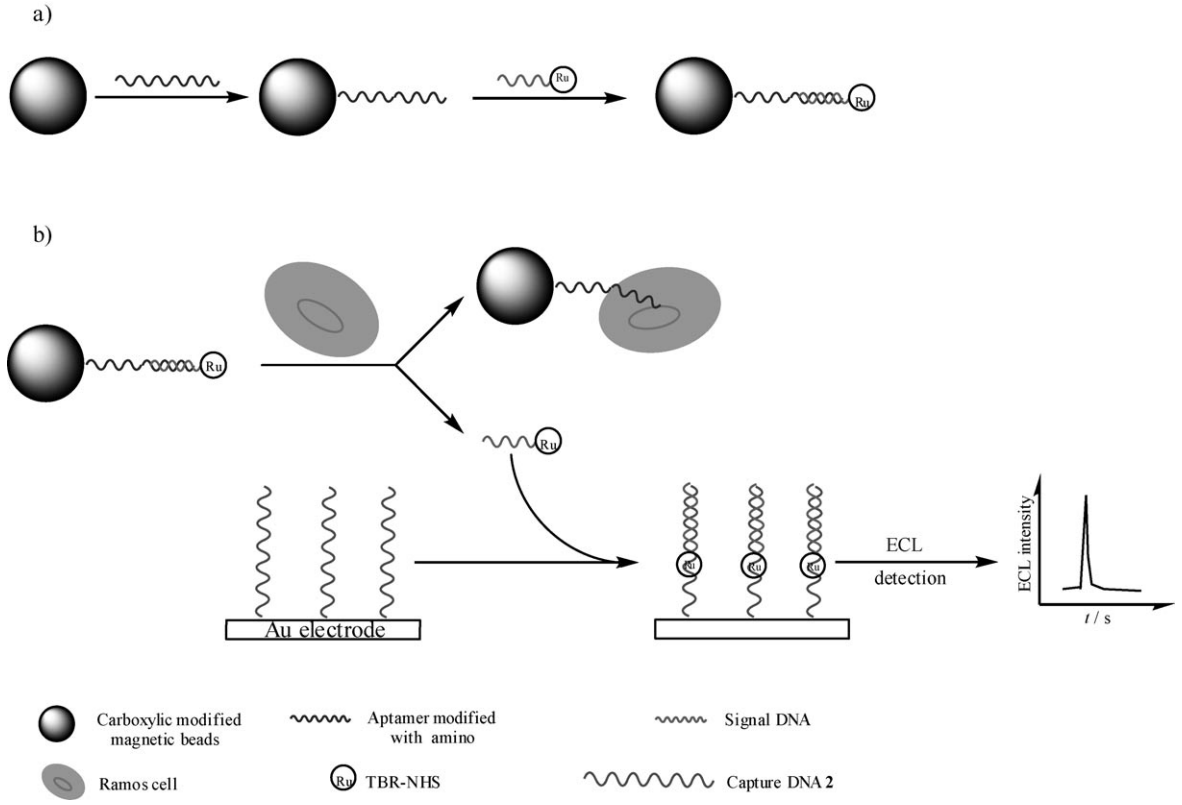

Scheme 2. Strategy for the MB-based ECL assay of Ramos cells.

without the signal amplification of NPs was almost the same as that with the electrochemical method. Investigations into the ECL detection of cancer cells by using aptamers and the signal amplification of NPs are underway in our lab. In addition, electrochemical detection by means of the MB–Au–CdS biocomplex proved successful for even complex samples such as FBS and demonstrated excellent sensitivity and selectivity. These assays have the potential to provide a simple, rapid, sensitive, and cost-effective approach for the early and accurate detection of cancer through the utilization of aptamers and nanotechnology.

Experimental Section

General: All of the synthetic oligonucleotides were purchased from SBS Genetech. (China). Sequences of the oligonucleotides are listed in Table 1.

Cells: Ramos cells (CRL-1596, B-cell, human Burkitt's lymphoma) were obtained from the Chinese Academy of Medical Sciences. The cells were cultured in RPMI 1640 medium supplemented with 10% fetal bovine serum (FBS) and 100 IU mL^{-1} penicillin Streptomycin. The cell density was determined by using a hemocytometer, and this was performed prior to any experiments. Approximately one million cells dispersed in RPMI 1640 cell media buffer were centrifuged at 3000 rpm for 5 min and redispersed in cell media three times and were then redispersed in cell media buffer (1 mL). During all experiments, the cells were kept in an ice bath at 4 °C.[32]

Preparation of Au NPs: Au NPs were prepared according to the method reported previously with a slight modification.[33] solutions of $HAuCl_4$ and trisodium citrate were filtered through a 0.22 μm microporous membrane filter prior to use, and then 1% trisodium citrate (1.0 mL) was added to a boiling 0.01% aqueous solution of $HAuCl_4$ (100 mL) and stirred for 10 min at the boiling point. The final Au NPs prepared by this method had an average diameter of approximately 30 nm measured by TEM, as shown in Figure S1 in the Supporting information. The prepared colloid gold NPs were stored in brown glass bottles at 4 °C.

Preparation of water-soluble CdS NPs: Mercaptoacetic acid modified CdS NPs were prepared according to the literature.[34] Briefly, MAA (2 μL) was added to a 1 mM aqueous solution of $CdCl_2$ (100 mL) under vigorous stirring, and the pH of the mixture was adjusted to around 11 with a 0.5 M aqueous solution of NaOH. After bubbling with N_2 for 30 min, a 1.34 mM aqueous solution of Na_2S (50 mL) was added dropwise to the solution. The reaction was carried out for 24 h under N_2 bubbling,

Table 1. The sequences of the DNA.

DNA	Sequence
aptamer for Ramos cells	5′-TAC AGA ACA CCG GGA GGA TAG TTC GGT GGC TGT TCA GGG TCT CCT CCC GGT G-SH (or NH_2)-3′
capture DNA **1**	5′-CGG TGT TCT GTA TTT TTT TTT TTT TTT TTT TTT TT–biotin-3′
linker DNA	5′-NH_2-TCT TTT TTC TTC TTA ACT CG-SH-3′
random DNA	5′-TAC AGA ACA CCG GCC GCT CAC ACG ATA TTT TTT TTG GAT CGA TCG TAC GA-SH-3′
signal DNA	5′-CGG TGT TCT GTA TTT TTT -NH_2-3′
capture DNA **2**	3′-GCC ACA AGA CAT AAA AAA TTT TTT TTT TTT TTT TTT TTT-SH -5′

and a Kelly colloid was formed gradually. Following centrifugation of the mixture for at least 30 min at 15000 rpm to remove the supernatant, the precipitate was washed and redispersed in water (30 mL) and stored at 4°C. The MAA-modified CdS NPs have an average diameter of about 10 nm measured by TEM as shown in Figure S2 in the Supporting Information.

Preparation of linker-DNA-labeled CdS nanoparticles: Linker DNA sequences were covalently labeled with MAA-modified CdS nanoparticles by using the following procedure: CdS colloid solution (10.0 mL) was centrifuged for 30 min at 10000 rpm, and the precipitate was redispersed in PBS buffer (5 mL). Then a 0.1 M aqueous solution of imidazole (200 μL; pH 6.8) was added to a 1.0×10^{-4} M solution of linker DNA (110 μL) for 30 min.[35] Then a 0.1 M aqueous solution of EDC (200 μL) and a solution of CdS (5 mL; pH 3.5) were added. The labeling reaction was stirred for 12 h at room temperature, and then centrifuged at 10000 rpm for 30 min at 4°C to remove unbound oligonucleotides. The linker-DNA–CdS conjugate was resuspended in PBS buffer (5 mL) and stored at 4°C after being washed twice with PBS buffer.

Preparation of the Au nanoprobes: The Au nanoprobes were prepared by following the published procedure.[36,37] First, the 30 nm Au particles were added to a solution containing the aptamers and the linker-DNA–CdS conjugates. The 3′-thiol-functionalized aptamers and linker DNA were activated with 10 mM TCEP at a ratio of 1:30. After shaking gently for 16 h, the solution was allowed to stand for another 40 h, followed by centrifugation for at least 30 min at 10000 rpm to remove excess reagents. Following removal of the supernatant, the precipitate was washed with PBS buffer, recentrifuged, and redispersed in PBS buffer (5 mL) and stored at 4°C. The TEM image of the Au NP probe is shown in Figure S3 in the Supporting Information.

Fabrication of the MB-Au-CdS biocomplex: The binding of the biotinylated capture DNA 1 with streptavidin-coated MBs was carried out by using a slightly modified procedure of that reported by Mascin et al.[38] First, streptavidin-coated MBs (40 μL) were transferred into a 1.5 mL Eppendorf tube and were washed three times with PBS buffer (500 μL; 10 mm phosphate, 0.1 m NaCl, pH 7.4), while physically retaining the particles with a magnetic field. Second, the MBs were resuspended in pH 7.4 PBS buffer (500 μL) and biotinylated capture DNA 1 (10 μL (from stock solution, 1.0×10−6 m) was added. The mixture solution was incubated for 1 h at 37°C with gentle shaking. The formed DNA 1-MB were separated from the incubation solution and washed three times with 500 μL of PBS buffer. The preparation process was followed by the resuspension of the DNA 1-MB in 200 μL PBS buffer, and then added 30 μL Au nanoprobes. After incubated at 37°C for 1 h, the formed MB-Au-CdS biocomplex were separated from the incubation solution and washed with PBS buffer for three times. The TEM of the biocomplex was shown in Figure S4 in the Supporting Information.

Synthesis of TBR-NHS ester: Ruthenium bis(2,2′-bipyridine)(2,2′-bipyridine-4,4′-dicarboxylic acid) *N*-hydroxysuccinimide ester (TBR-NHS ester) was prepared according to a previously published procedure.[37,38] To synthesize $[Ru(bpy)_2Cl_2]$, first, $RuCl_3{\cdot}xH_2O$ (0.0998 g) was reacted with a twofold excess of the 2,2′-bipyridine (0.1581 g) under reflux in ethyl glycol (10 mL) for 6 h. The solution was cooled to room temperature and extracted with acetone (5 mL) and diethyl ether (20 mL) until the ethyl glycol was completely transferred to the diethyl ether phase. The resulting solid was dissolved in ethanol and then filtered.

Synthesis of $[Ru(bpy)_2(dcbpy)(PF_6)_2]$: This synthesis was performed according to the procedure reported previously.[38,39]The as-prepared $[Ru(bpy)_2Cl_2]$ (0.16 g), $NaHCO_3$(0.16 g), and 2,2′-bipyridine-4,4′-dicarboxylic acid (0.12 g) were added to a solution of methanol and H_2O solution (20 mL; 4:1 v/v) and the stirred solution was heated for 4 h. The solution was cooled in an ice bath for 7 h, and the pH of the solution was adjusted with hydrochloric acid to pH 4.4. The formed precipitate was filtered and washed with methanol. $NaPF_6$ (2.0 g) in water (14 mL) was added to the resulting filtrate, and then cooled in an ice bath. The formed precipitate was collected by filtration, and dried.

Dicyclohexylcarbodiimide (0.23 g) and *N*-hydrosuccinimide (0.119 g) were dissolved in DMF (1.5 mL) with stirring and cooled in an ice bath. DMF (1 mL) containing $[Ru(bpy)_2(dcbpy)][PF_6]_2$ (0.1532 g) was added, and the mixture was stirred for 5 h to form $[Ru(bpy)_2(dcbpy)NHS]$.

Preparation of ECL probe: The ECL probe was synthesized according to a slightly modified literature procedure.[40] A 5.84×10^{-4} M solution of TBR-NHS ester (200 μL) and 0.10 M tetraborate buffer (10 μL; pH 8.50) was added to the 1.0×10^{-4} M solution of signal DNA (50 μL), respectively, allowed to shake at low speed overnight at room temperature. Then, by addition of a 3 M solution of NaAc (100 μL) and ethanol (2 mL) to the mixture, the precipitate reaction was carried out in the refrigerator at ≤ -20°C for 12 h. The mixture was centrifuged in a micro-centrifuge at 12000 rpm for 30 min. The supernatant was carefully removed and the precipitate was rinsed with cold 70% ethanol twice and dried in air. The dried precipitate was redissolved in 1.0 M PBS buffer (200 μL; pH 7.0, 0.10 M NaCl + 1.0 M KH_2PO_4/K_2HPO_4) and stored at −16°C in refrigerator. The resulting solution was used as a stock solution for the ECL probe.

Fabrication of the MB-Ru biocomplex: The binding of the amino-modified aptamers with carboxyl-group-coated MBs was carried out by using a slightly modified literature procedure.[41] First, carboxyl-group-coated MBs (40 μL) were transferred into a 1.5 mL Eppendorf tube and were washed three times with PBS buffer (500 μL; 10 mM phosphate, 0.1 M NaCl, pH 7.4), while physically retaining the particles with a magnetic field. Then, a 0.1 M solution of EDC (150 μL) was added to the MBs for 40 min to activate the MBs. Second, the MBs were washed and resuspended in a 1.0×10^{-6} M solution of amino-modified aptamer (100 μL). The resulting MBs and aptamer solution were incubated for 12 h at 37°C with gentle shaking. The formed MB–aptamer conjugates were separated from the incubation solution and washed three times with PBS buffer (500 μL). The preparation process was followed by the resuspension of the MB–aptamer conjugate in PBS buffer (100 μL), and then ECL probes (30 μL) were added. The mixture was incubated at 37°C for 1 h. The formed MB–Ru biocomplex was separated from the incubation solution and washed with PBS buffer three times.

Finally, the MB–Ru biocomplex was incubated with PBS buffer (300 μL) containing different numbers of cells at room temperature for 120 min. Then the ECL probes released from the MB–Ru biocomplex were separated from the solution with a magnetic field and used to hybridize with the capture DNA 2 on the gold electrode in the subsequent step.

Electrochemical detection: The MB-Au-CdS biocomplexes were incubated with PBS buffer (300 μL) containing different numbers of cells at room temperature for 120 min. Then the solution separated from the mixture was added to a 1.0 M aqueous solution of HNO_3 (200 μL). After mixing for 5 min, the dissolved Cd^{2+} solution was transferred into 2.5 mL of the 0.1 M pH 5.3 HAC-NaAC buffer supporting electrolyte solution containing 1.8×10^{-4} M $HgCl_2$. A control experiment was performed by a similar fashion but without the target cells.

Stripping voltammetric measurements of the dissolved Cd^{2+} were performed (in a stirring HAC-NaAC buffer solution) by using an in situ preparation of mercury film on a glassy carbon electrode with a deposition time of 300 s and deposition potential of −1.4 V. The positive differential pulse voltammetry (DPV) scan was performed after a 15 s rest period (without stirring) from −0.8 to −0.5 V (vs. Ag/AgCl), with a pulse amplitude of 50 mV and a pulse width of 50 ms. The anodic stripping peak current ($i_{p,a}$) located at ca. −0.62 V was taken as the analytical response.

Electrochemiluminescence (ECL) detection: The surface of the gold electrode was pretreated step by step in the following order: heated in a piranha solution (30% H_2O_2: concentrated H_2SO_4 3:7) for about 5 min to remove any previous organic layer, polished with alumina slurries (1, 0.3, and 0.05 μm in turn) to obtain a mirrorlike surface, washed ultrasonically with deionized and doubly distilled water, dried with nitrogen gas and cycled in a 0.5 M aqueous solution of H_2SO_4 scanning between 0.3 and 1.5 V until a stable gold oxide formation/reduction cyclic voltammogram was obtained. The cleaned Au electrode was immersed in 1.0×10^{-6} M capture DNA 2 solution (100 μL) for 12 h to obtain a capture-DNA 2–immobilized electrode. Loosely adsorbed capture DNA 2 was removed by washing carefully with 10 mM PBS buffer. Then the capture DNA 2 immobilized electrode was immersed into a 1.0 M solution of MCH (100 μL)

for 30 min to eliminate nonspecific adsorption and then washed carefully with 10 mM PBS. Finally, the preparation process was followed by immersion of the capture-DNA 2-modified electrode into the solution containing the ECL probe, released from the MB–Ru biocomplexes in the presence of the Ramos cells, for 1 h at 37 °C to form ds-DNA. The electrode was sequentially washed with 10 mM PBS to removed the unbinding the ECL probe.

The ECL measurement was performed at a constant potential of +1.0 V in 0.10 M PBS buffer (2.0 mL; pH 7.4) containing 0.10 M TPA. And the chronoamperometry (CA) was determined by measuring the ECL signal.[42]

Cell imaging: Fluorescence imaging was conducted with a fluorescence microscope setup consisting of an Nikon E 800 inverted microscope with an Nikon Digital sight DS-U1 camera. The fluorescent NPs were excited at 400 nm, and emission was detected at 545 nm.

Acknowledgements

This work was supported by the National Nature Science Foundation of China (No. 20975059), the National Nature Science Foundation of Shandong Province (no. ZR2009BZ005), and the National Basic Research Program of China (no. 2010CB732404).

[1] F. A. Vlems, T. J. Ruers, C. J. Punt, T. Wobbes, G. N. van Muijen, *Eur. J. Surg.* **2003**, *29*, 289–302.
[2] P. Paterlini-Brechot, N. L. Benali, *Cancer Lett.* **2007**, *253*, 180–204.
[3] K. Pantel, U. Woelfle, *Biochim. Biophys. Acta Rev. Cancer* **2005**, *1756*, 53–64.
[4] V. Zieglschmid, C. Hollmann, O. Bocher, *Crit. Rev. Clin. Lab. Sci.* **2005**, *42*, 155–196.
[5] S. Mocellin, U. Keilholz, C. R. Rossi, D. Nitti, *Trends Mol. Med.* **2006**, *12*, 130–139.
[6] S. Faderl, H. M. Kantarjian, M. Talpaz, Z. Estrov, *Blood* **1998**, *91*, 3995–4019.
[7] R. Paredes-Aguilera, *Am. J. Hematol.* **2001**, *68*, 69–74.
[8] L. Belov, O. de La Vega, C. G. dos Remedios, S. P. Mulligan, R. I. Christopherson, *Cancer Res.* **2001**, *61*, 4483–4489.
[9] R. A. Ghossein, S. Bhattacharya, *Eur. J. Cancer* **2000**, *36*, 1681–1694.
[10] H. Iinuma, K. Okimaga, M. Adachi, K. Suda, T. Sekine, K. Sakagawa, Y. Baba, J. Tamura, H. Kumagai, A. Ida, *Int. J. Cancer* **2000**, *89*, 337–344.
[11] J. A. Liu Yin, D. Grimwade, *Lancet* **2002**, *360*, 160–162.
[12] D. Du, H.-X. Ju, X.-J. Zhang, J. Chen, J. Cai, H.-Y. Chen, *Biochemistry* **2005**, *44*, 11539–11545.
[13] C. Hao, L. Ding, X.-J. Zhang, H.-X. Ju, *Anal. Chem.* **2007**, *79*, 4442–4447.
[14] W. Cheng, L. Ding, J.-P. Lei, S.-J. Ding, H.-X. Ju, *Anal. Chem.* **2008**, *80*, 3867–3872.
[15] L. Ding, W. Cheng, X.-J. Wang, S.-J. Ding, H.-X. Ju, *J. Am. Chem. Soc.* **2008**, *130*, 7224–7225.
[16] L. Gold, B. Polisky, O. Uhlenbeck, M. Yarus, *Rev. Annu. Biochem.* **1995**, *64*, 763.
[17] E. N. Brody, L. Gold, *Rev. Mol. Biotechnol.* **2000**, *74*, 5–13.
[18] D. S. Wilson, J. W. Szostak, *Rev. Annu. Biochem.* **1999**, *68*, 611.
[19] S. D. Jayasena, *Clin. Chem.* **1999**, *45*, 1628.
[20] R. Kirby, E. J. Cho, B. Gehrke, T. Bayer, Y. S. Park, D. P. Neikirk, J. T. McDevitt, A. D. Ellington, *Anal. Chem.* **2004**, *76*, 4066–4075.
[21] I. German, D. D. Buchanan, R. T. Kennedy, *Anal. Chem.* **1998**, *70*, 4540–4545.
[22] S. E. Osborne, I. Matsumura, A. D. Ellington, *Curr. Opin. Chem. Biol.* **1997**, *1*, 5–9.
[23] O. C. Farokhzad, S. Jon, A. Khademhosseini, T. T. Tran, D. A. LaVan, R. Langer, *Cancer Res.* **2004**, *64*, 7668–7672.
[24] D. A. Daniels, H. Chen, B. J. Hicke, K. M. Swiderek, L. Gold, *Proc. Natl. Acad. Sci. USA* **2003**, *100*, 15416–15421.
[25] K. H. Joshua, E. S. Joshua, D. M. Colin, D.-H. Shangguan, W.-H. Tan, *Anal. Chem.* **2006**, *78*, 2918–2924.
[26] E. S. Joshua, D. M. Colin, Z.-W. Tang, D.-H. Shangguan, L. Charles, W.-H. Tan, *Anal. Chem.* **2007**, *79*, 3075–3082.
[27] Y.-F. Huang, H.-T. Chang, W.-H. Tan, *Anal. Chem.* **2008**, *80*, 567–572.
[28] D. M. Colin, E. S. Joshua, Z.-W. Tang, Y.-R. Wu, B. Suwussa, W.-H. Tan, *Anal. Chem.* **2008**, *80*, 1067–1072.
[29] Y. Chen, C. M. Alina, Y.-F. Huang, P. Joseph, Z. Zhu, M. Michael, W.-H. Tan, *Chem. Eur. J.* **2009**, *15*, 5327–5336.
[30] Z.-Y. Xiao, D.-H. Shangguan, Z.-H. Cao, X.-H. Fang, W.-H. Tan, *Chem. Eur. J.* **2008**, *14*, 1769–1775.
[31] S. S. Zhang, H. Zhong, C. F. Ding, *Anal. Chem.* **2008**, *80*, 7206–7212.
[32] D. M. Colin, E. S. Joshua, Z.-W. Tang, Y.-R. Wu, B. Suwussa, W.-H. Tan, *Anal. Chem.* **2008**, *80*, 1067–1072.
[33] K. C. Grabar, P. C. Smith, M. D. Musick, J. A. Davis, D. G. Walter, M. A. Jackson, A. P. Guthrie, M. J. Natan, *J. Am. Chem. Soc.* **1996**, *118*, 1148–1153.
[34] T. N. Milica, I. C. Mirjana, V. Veana, I. M. Olga, *J. Phys. Chem.* **1990**, *94*, 6390–6396.
[35] Y. Xu, Y. Cai, P. G. He, Y. Z. Fang, *Electroanalysis* **2004**, *16*, 150–155.
[36] J.-M. Nam, S. I. Stoeva, C. A. Mirkin, *J. Am. Chem. Soc.* **2004**, *126*, 5932–5933.
[37] J. J. Storhoff, R. Elghanian, C. R. Mucic, C. A. Mirkin, L. R. Letsinger, *J. Am. Chem. Soc.* **1998**, *120*, 1959–1964.
[38] S. Centi, S. Tombelli, M. Mascin, M. Minunni, *Anal. Chem.* **2007**, *79*, 1466–1473.
[39] E. Terpetschnig, H. Szmacinski, H. Malak, J. R. Lakowicz, *Biophys. J.* **1995**, *68*, 342–350.
[40] T. Shimidzu, K. Iyoda, *J. Phys. Chem.* **1985**, *89*, 642–645.
[41] J. Miao, Z. Cao, Y. Zhou, C. Lan, J. Lu, *Anal. Chem.* **2008**, *80*, 1606–1613.
[42] J. Zhang, H. Qi, Y. Li, J. Yang, Q. Gao, C. Zhang, *Anal. Chem.* **2008**, *80*, 2888–2894.

Received: May 2, 2010
Published online: July 23, 2010

